UUITP-01/16

Heavy photophilic scalar at the LHC from a varying electromagnetic coupling

Ulf Danielsson,* Rikard Enberg,† Gunnar Ingelman,‡ and Tanumoy Mandal§

Department of Physics and Astronomy,

Uppsala University, Box 516, SE-751 20 Uppsala, Sweden

(Dated: October 14, 2016)

arXiv:1601.00624v3 [hep-ph] 13 Oct 2016

Abstract

We investigate the phenomenology of a heavy scalar ϕ of the type involved in Bekenstein's framework for varying electromagnetic coupling theories, with the difference that the scalar in our model has a large mass. The model has only two free parameters, the mass M_ϕ of the scalar and the scale Λ of new physics. The scalar is dominantly produced through photon-photon fusion at the LHC and leads to a diphoton final state. It can also be produced by quark-antiquark fusion in association with a photon or a fermion pair. Its dominating decay is to diphotons, but it also has a large three-body branching to a fermion pair and a photon, which can provide an interesting search channel with a dilepton-photon resonance. We derive exclusion limits on the $M_\phi - \Lambda$ plane from the latest 13 TeV LHC diphoton resonance search data. For a benchmark mass of $M_\phi \sim 1$ TeV, we find a lower limit on Λ of 18 TeV. We discuss the more complex possibility of varying couplings in the full electroweak theory and comment on the possibility that the new physics is related to extra dimensions or string theory.

* ulf.danielsson@physics.uu.se

† rikard.enberg@physics.uu.se

‡ gunnar.ingelman@physics.uu.se

§ tanumoy.mandal@physics.uu.se

I. INTRODUCTION

In this paper we perform the first ever study of the collider physics of a model for space-time-varying gauge couplings. The model we study was constructed almost thirty-five years ago by Jacob Bekenstein [1, 2] and introduces a new scalar field associated with a variation in the electromagnetic (EM) coupling constant ($\alpha_{\rm EM}$). This model has, to the best of our knowledge, previously only been studied in the context of cosmology with a massless, or very light, scalar, and bounds on the model have been considered based on low-energy physics and astrophysics, see e.g. [3]. Here we propose that the Bekenstein model can be relevant for particle physics experiments, and that the scalar can have a mass on the TeV scale and therefore be accessible at the LHC.

Bekenstein's model is the first consistent such model – it is Lorentz, gauge and time-reversal invariant and respects causality. The original motivation was to accommodate possible variations of the fine-structure constant over cosmological scales, but despite careful searches such variations have not been detected [3].

In string theory all couplings are associated with scalar fields called moduli, and are thus subject to variations. The excitations of these fields are typically very heavy and as a consequence the couplings will be locked to essentially constant values, given by the specific compactification scenario, see e.g. [4] for a discussion. The Bekenstein model is not derived from string theory, but we consider it the simplest consistent scenario for associating couplings with scalar fields.

Recently both the ATLAS and the CMS collaborations reported excesses in the diphoton invariant mass distribution around 750 GeV based on the 13 TeV data with ~ 3 fb^{-1} integrated luminosity [5, 6]. When the larger dataset with ~ 16 fb^{-1} integrated luminosity was analyzed no excess was observed [7, 8]. The previously observed excesses had local significances of $3.6 - 3.9\sigma$ for ATLAS and $2.0 - 2.6\sigma$ for CMS depending on the width of the resonance [5, 6]. The global significances, including the look-elsewhere effect, were slightly lower, but the fact that both experiments observed the same kind of excess at the same value of the diphoton invariant mass generated a large amount of theoretical activity, see e.g. [9–127].

In the first version of the present paper,[1] which was submitted shortly after the an-

[1] Available as arXiv:1601.00624v2

nouncement of the observed excess, we proposed that the diphoton excess could be explained by a massive scalar of the type appearing in the Bekenstein model. The 750 GeV excess was thus the original reason that we began to study the LHC phenomenology of the model. However, our model is unique and is therefore interesting on its own, even though the previous excess has faded away. Therefore, we will in this new version of the paper instead begin a study of the more general LHC phenomenology of the model, by using the new data to set constraints on the model parameters. In a forthcoming publication [128] we will continue these studies.

Our model is fundamentally different from other beyond Standard Model (BSM) theories discussed as possibilities for new physics phenomena to be observed at the LHC. The variation of $\alpha_{\rm EM}$ implies that the new scalar field ϕ couples to photons, i.e., it is photophilic. This favors its decay to two photons, which is essential in connection with the mentioned diphoton resonance searches, but it also favors its production through photon-photon ($\gamma\gamma$) fusion rather than through gluon-gluon (gg) fusion as is more commonly considered for new scalars in BSM theories. Although the scalar in our model can be produced in a pure s-channel process, the basic new vertices also give production modes together with a photon or a dijet or dilepton pair, which imply characteristic predictions of the model to be tested against data.

Our model is also economic in the sense that it introduces only one new field and two new parameters, i.e., the scalar ϕ with mass M_ϕ, and the new energy scale Λ. With M_ϕ around the electroweak (EW) or TeV scale, $\alpha_{\rm EM}$ remains constant throughout most of the history of the universe and no deviations would have been detectable so far.[2] An observation of this scalar would then be the first hint that $\alpha_{\rm EM}$ can vary if the energy is high enough.

This paper is organized as follows. In Section II we introduce the model and derive the interactions of the new scalar. We also discuss briefly the generalization to the whole EW sector of the SM. In Section III we discuss the phenomenology of the model, and through detailed numerical comparison with LHC limits we extract bounds on the model parameters in Section IV. In Section V we conclude by considering the results in a larger context.

[2] The new scalar should also be investigated as a candidate for the inflaton. The quadratic contribution to the potential, with a TeV scale mass cannot be used for inflation, but one might consider higher order terms providing a useful shape.

II. THE MODEL

In the Bekenstein model [1, 2] the variation of the coupling e is derived from an action that reduces to electromagnetism for constant coupling. It is assumed that the space-time variation of the coupling is given by $e = e_0\epsilon(x)$, where $\epsilon(x)$ is a scalar field with dynamics given by the kinetic term

$$\frac{1}{2}\frac{\Lambda^2}{\epsilon^2}(\partial_\mu\epsilon)^2, \tag{1}$$

where Λ is an energy scale. It is assumed that the field ϵ multiplies the electric charge e everywhere in the Lagrangian of the model. Specifically, this means that eA_μ is everywhere replaced by $e_0\epsilon A_\mu$. Gauge invariance, and invariance with respect to a rescaling of ϵ, then requires that the field strength tensor be given by

$$F_{\mu\nu} = \frac{1}{\epsilon}\left[\partial_\mu(\epsilon A_\nu) - \partial_\nu(\epsilon A_\mu)\right]. \tag{2}$$

To keep our notation as explicit as possible we define $\widehat{F}_{\mu\nu} = \partial_\mu A_\nu - \partial_\nu A_\mu$, and introduce a scalar field φ such that $\epsilon = e^\varphi$. We will be assuming small fields, working at lowest order, and therefore write $\epsilon \simeq 1 + \varphi$, and keep only terms linear in φ. We then find, for the kinetic term of the field, that $F_{\mu\nu}F^{\mu\nu} = \widehat{F}_{\mu\nu}\widehat{F}^{\mu\nu} + 4\,\partial_\mu\varphi\, A_\nu\widehat{F}^{\mu\nu}$. Finally, we define a new field $\phi = \varphi\Lambda$ so that all fields have their usual mass dimensions. In this way we find a Lagrangian for electromagnetism plus the scalar field given by

$$\mathcal{L} \supset \frac{1}{2}(\partial_\mu\phi)^2 - \frac{1}{4}\widehat{F}_{\mu\nu}\widehat{F}^{\mu\nu} - \frac{1}{\Lambda}\partial_\mu\phi\, A_\nu\widehat{F}^{\mu\nu}. \tag{3}$$

It is shown in [1], see also [129], that one through a partial use of the equation of motion for $F_{\mu\nu}$ can map the theory to a new theory where the scalar only couples through $(1/2\Lambda)\phi\widehat{F}_{\mu\nu}\widehat{F}^{\mu\nu}$, without any coupling between the scalar and the fermions. These theories are equivalent, and we here consider the original action due to Bekenstein.

Because of the definition of e, the new scalar field ϕ will in addition to the interaction in Eq. (3) couple to all electrically charged fields. The coupling of the EM field to charged fermions is obtained from the covariant derivative, which is given by $D_\mu = \partial_\mu - ieQA_\mu$, where Q is the charge of the coupled field, and $e = e_0\epsilon$ so that $D_\mu = \partial_\mu - ie_0QA_\mu - ie_0Q(\phi/\Lambda)A_\mu$. If we now define $\widehat{D}_\mu = \partial_\mu - ie_0QA_\mu$ as the more familiar covariant derivative of electromagnetism, the gauge invariant kinetic term for fermions is given by

$$\mathcal{L} \supset i\overline{\psi}\not{D}\psi = i\overline{\psi}\not{\widehat{D}}\psi + \frac{e_0Q}{\Lambda}\phi\,\overline{\psi}\gamma^\mu\psi\, A_\mu. \tag{4}$$

The final interaction of ϕ to consider is the coupling to $W^\pm$ bosons, which is obtained by inserting $eA_\mu = e_0\epsilon A_\mu$ in the EW gauge kinetic term written in terms of the mass eigenstates. The resulting terms to lowest order in the electric coupling are shown below in Eq. (5).

As we have described above, this model has been used as a framework for a space-time varying $\alpha_{\rm EM}$ with a massless or very light scalar field ϕ. We will now add one new ingredient: a mass term for the scalar field with M_ϕ around the EW scale or up to several TeV. The energy cost of moving ϕ away from its minimum will then be very large for energies $\lesssim M_\phi$, so that $\alpha_{\rm EM}$ will have negligible variation.

To get the Lagrangian in its final form, let us now drop the hats on the above expressions, so that from now on, $F_{\mu\nu}$ is the standard field strength tensor. Collecting all terms, we then have the Lagrangian of our model

$$\begin{aligned}\mathcal{L} = \mathcal{L}_{\rm SM} &+ \frac{1}{2}(\partial_\mu\phi)^2 - \frac{1}{2}M_\phi^2\phi^2 - \frac{1}{\Lambda}\partial_\mu\phi\, A_\nu F^{\mu\nu} + \frac{e_0 Q}{\Lambda}\phi\,\overline{\psi}\gamma^\mu\psi\, A_\mu \\ &+ \frac{ie_0}{\Lambda}\phi\left[W^+_{\mu\nu}W^{-\mu}A^\nu - W^-_{\mu\nu}W^{+\mu}A^\nu + F^{\mu\nu}W^+_\mu W^-_\nu\right] \\ &+ \frac{ie_0}{\Lambda}\left[(A_\nu\partial_\mu\phi - A_\mu\partial_\nu\phi)W^+_\mu W^-_\nu\right], \end{aligned} \tag{5}$$

where $\mathcal{L}_{\rm SM}$ represents the ordinary Standard Model Lagrangian, $W^\pm_{\mu\nu} = \partial_\mu W^\pm_\nu - \partial_\nu W^\pm_\mu$ and ψ is a generic field with charge Q denoting all electrically charged fermions of the Standard Model, written as Dirac spinors for both left- and right-handed components. Thus our model has only two new parameters, the mass M_ϕ and the scale Λ. Note that the EM coupling e_0 in Eq. (5) is the usual not varying coupling, and the dynamics of the varying constant now sit instead in the scalar field ϕ.[3]

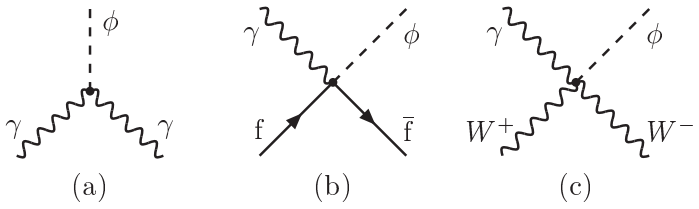

FIG. 1. Basic interaction vertices of the scalar field ϕ as given by the Lagrangian in Eq. (5).

[3] For example, at very high energies above the mass of ϕ, small variations of the coupling constant e could become visible in e^+e^- collisions at a future linear collider. In the formulation here, where we have the fixed constant e_0, such variations would be associated with loops or real or virtual emission diagrams involving ϕ.

The last three terms in Eq. (5) are interaction terms. The vertices are shown in Fig. 1 and the corresponding Feynman rules are

$$\text{Fig. 1a} \quad : \quad \gamma\gamma\phi \quad \to \frac{i}{\Lambda}\left(p_{1\mu}p_{3\nu} + p_{3\mu}p_{2\nu} + g_{\mu\nu}\, p_3 \cdot p_3\right) \tag{6}$$

$$\text{Fig. 1b} \quad : \quad \mathrm{f\bar{f}}\gamma\phi \quad \to \frac{ie_0 Q}{\Lambda}\gamma^\mu \tag{7}$$

$$\begin{aligned}\text{Fig. 1c} : \quad \gamma\phi W^+W^- \to \frac{ie_0}{\Lambda}&\left(p_1^{\mu_3} g_{\mu_1,\mu_4} - p_1^{\mu_4} g_{\mu_1,\mu_3} + p_2^{\mu_3} g_{\mu_1,\mu_4} - p_2^{\mu_4} g_{\mu_1,\mu_3}\right.\\ &\left. + p_3^{\mu_4} g_{\mu_1,\mu_3} - p_3^{\mu_1} g_{\mu_3,\mu_4} + p_4^{\mu_1} g_{\mu_3,\mu_4} - p_4^{\mu_3} g_{\mu_1,\mu_4}\right),\end{aligned} \tag{8}$$

where in (6) and (8) the numbered indices refer to the particles in the order listed.

For simplicity, we have only let the EM coupling e vary. This has the consequence that only the photon and the fields carrying electric charge couple to ϕ. It is possible to instead let the $\mathrm{U}(1)_Y$ or $\mathrm{SU}(2)_L$ or both couplings vary, which will couple the ϕ not only to the photons but to the weak gauge bosons as well. The Bekenstein model of varying-α_{EM} theory has been generalized [130] to vary the $\mathrm{SU}(2)_L$ and $\mathrm{U}(1)_Y$ couplings of the electroweak (EW) theory, either with both couplings varying in the same way (one scalar field associated with both variations), or independently of each other. In the latter case, there will be two scalar fields associated with the variations of the two gauge couplings.

Let us therefore here briefly consider the extension of the model to the entire electroweak gauge group. We will perform a detailed study of this extension in a forthcoming paper [128]. Consider, therefore, two scalars S and S' associated with the variation of g and g', where g and g' are the $\mathrm{SU}(2)_L$ and $\mathrm{U}(1)_Y$ gauge couplings respectively. The interaction Lagrangian (before EWSB) can be expressed as (for simplicity using the equivalent formulation discussed in connection with Eq. (3))

$$\mathcal{L} \supset \frac{1}{2\Lambda} S B_{\mu\nu} B^{\mu\nu} + \frac{1}{2\Lambda'} S' W_{\mu\nu} W^{\mu\nu} \ , \tag{9}$$

where $B_{\mu\nu}$ and $W_{\mu\nu}$ are the field-strength tensors and Λ and Λ' are the scales for the $\mathrm{SU}(2)_L$ and $\mathrm{U}(1)_Y$ gauge groups respectively. In Eq. (9), we now replace $B_\mu = c_w A_\mu - s_w Z_\mu$ and $W^3_\mu = s_w A_\mu + c_w Z_\mu$ where s_w and c_w are the sine and cosine of the Weinberg angle, respectively. After this replacement, we obtain

$$\mathcal{L} \supset \frac{1}{2}\left(c_w^2 \frac{S}{\Lambda} + s_w^2 \frac{S'}{\Lambda'}\right) F_{\mu\nu}F^{\mu\nu} + \frac{1}{2}\left(s_w^2 \frac{S}{\Lambda} + c_w^2 \frac{S'}{\Lambda'}\right) Z_{\mu\nu}Z^{\mu\nu} - s_w c_w \left(\frac{S}{\Lambda} - \frac{S'}{\Lambda'}\right) F_{\mu\nu}Z^{\mu\nu}. \tag{10}$$

The fields S and S' need not be the mass eigenstates, which in general could be linear combinations of S and S'. We therefore define the mass eigenstates ϕ and ϕ' as

$$\phi = \alpha S + \alpha' S'; \quad \phi' = \beta S + \beta' S' \ , \tag{11}$$

where α, β, α' and β' are parameters determined from the free parameters of the scalar potential (which we will not present here). We may identify ϕ as the lightest scalar and ϕ' as a heavier mass eigenstate by properly arranging various free parameters in the scalar potential. In the following, we only focus on the lightest scalar, which may reasonably be expected to first show up at the LHC, and assume that signatures of the heavier will be detected later.[4] In this general set-up, both ϕ and ϕ' will decay to $\gamma\gamma$, γZ and ZZ modes. Neglecting the small phase-space suppression for the heavy gauge bosons in the final state, the two-body branching ratios (BRs) of ϕ are in the following proportions,

$$\mathrm{BR}_{\gamma\gamma} : \mathrm{BR}_{\gamma Z} : \mathrm{BR}_{ZZ} \approx \frac{1}{2}\left(\alpha c_w^2 + \beta s_w^2\right)^2 : s_w^2 c_w^2 \left(\alpha - \beta\right)^2 : \frac{1}{2}\left(\alpha s_w^2 + \beta c_w^2\right)^2 . \tag{12}$$

For example, the no mixing case, i.e., $\alpha = 1$ and $\beta = 0$, results in

$$\mathrm{BR}_{\gamma\gamma} : \mathrm{BR}_{\gamma Z} : \mathrm{BR}_{ZZ} \approx \frac{1}{2}c_w^4 : s_w^2 c_w^2 : \frac{1}{2}s_w^4 \approx 60\% : 35\% : 5\% \tag{13}$$

There is a substantial parameter range where the $\gamma\gamma$ decay dominates and the γZ and ZZ decays are suppressed and therefore not observable with presently available data samples. In this first study, it is therefore well motivated to find the most essential phenomenology of this varying coupling theory by the simplification to only vary the EM coupling. Thus, we leave the more complex study of the full theoretical framework for future work [128].

III. DECAYS AND PRODUCTION AT THE LHC

In this section, we study the phenomenology of our model and derive limits on the two model parameters M_ϕ and Λ from the relevant 8 and 13 TeV data from the LHC. In particular, we use $\gamma\gamma$ [7, 8], γZ [131, 132] and ZZ [133] resonance searches from the LHC. The $\gamma\gamma$ data are used for the simplified model where ϕ only couples to photons, but all three types of data are used to set limits on the varying EW theory. We implement

[4] Of course, the two scalars may also be close in mass. We will consider this possibility in the future.

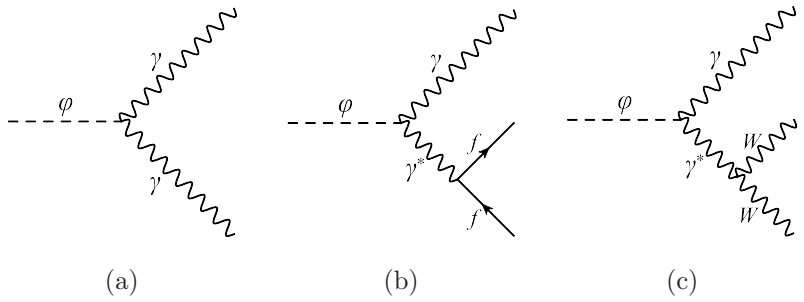

FIG. 2. Sample Feynman diagrams of the two and three-body decay modes of ϕ.

the Lagrangian shown in Eq. (5) in FeynRules2 [134] to generate the model files for the MadGraph5 [135] event generator. We use the MMHT14LO [136] parton distribution functions (PDFs) to compute cross sections. Generated events are passed through Pythia8 [137] for parton shower and hadronization. Detector simulation is performed for ATLAS and CMS using Delphes3 [138] which uses the FastJet [139] package for jet clustering using the anti-k_T algorithm [140] with clustering parameter $R = 0.4$.

Since ϕ originates from the variation of the fine-structure constant, it directly couples to photons through an effective dimension-5 operator of the type $\phi F_{\mu\nu}^2$. The only possible two-body decay of ϕ is the diphoton mode (Fig. 2a), which is a tree level decay – not a loop-induced decay through a charged particle as for the SM Higgs. There are subdominant three-body decays of ϕ mediated through an off-shell photon as shown in Figs. 2b and 2c. There are also subdominant four-body decay modes for ϕ (*e.g.* $\phi \to \gamma\psi^+\psi^{-*} \to \gamma\gamma\psi^+\psi^-$). The partial decay width into two photons, shown in Fig. 2a, is given by

$$\Gamma(\phi \to \gamma\gamma) = \frac{M_\phi^3}{16\pi\Lambda^2}. \tag{14}$$

The analytical expressions for the subdominant multi-body decay modes are more complicated due to massive particles in the three-body phase space, and we compute partial widths of those modes numerically in MadGraph5. In Table I, we show the partial widths and branching ratios (BR) of ϕ into its two, three and four body decay modes for $M_\phi = 1$ TeV and $\Lambda = 2$ TeV, calculated numerically. It is important to note that the BRs of ϕ only depend on its mass but are independent of the scale Λ. This is because all partial widths and hence the total width scale as Λ^{-2} and the Λ dependence cancels in the ratios. From Table I, we can see that $\phi \to \gamma\gamma$ is the dominant decay mode and this mode has a branching ratio of about 60%. But BRs of ϕ to other modes are non-negligible. In

Decay Mode	$\phi \to \gamma\gamma$	$\phi \to \gamma ff(jj)$	$\phi \to \gamma\gamma ff$	$\phi \to \gamma WW$	$\phi \to \gamma\gamma WW$	Total
Width (GeV)	4.973	1.851 (0.859)	0.414	0.794	0.053	8.085
BR (%)	61.5	22.9 (10.6)	5.12	9.82	0.66	-

TABLE I. The partial widths and BRs of ϕ for $M_\phi = 1$ TeV. The widths are proportional to Λ^{-2} and are here given for $\Lambda = 2$ TeV, whereas the BRs are independent of Λ. Here, f includes all SM charged fermions and j denotes jets of "light" quarks, including b quarks. The four-body final states are non-negligible corrections to the three-body modes.

our analysis we always use the total decay width including all contributions coming from the three and four body decays.

In Fig. 3, we show a few sample Feynman diagrams of the main production channels of ϕ at the LHC. Unlike the gg initiated SM-like Higgs boson production, these channels are induced by $\gamma\gamma$, γq and qq initial states. The dominant production channel of ϕ is the $\gamma\gamma$ fusion where the initial photons come from the photon distribution of the proton. In the $\gamma\gamma$ fusion process, the dominant contribution comes from inelastic scattering, where the proton would break up. On the other hand, elastic collisions, where the proton will remain intact, are subdominant but provide a much cleaner channel that can be identified with forward detectors. This exclusive production of ϕ, i.e. $pp \to \phi pp$, where two forward protons are tagged, is an interesting process to search for (this production mode has been considered in [141–143], for models very different from ours). In Table II, we present the partonic cross sections of various production modes of ϕ for the 8 and 13 TeV LHC for $M_\phi = 1$ TeV and $\Lambda = 2$ TeV. To compute these cross sections we apply the following

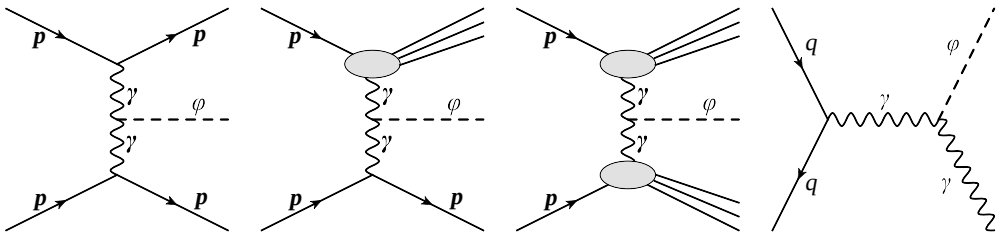

(a) (b) (c) (d)

FIG. 3. Sample Feynman diagrams of the production of ϕ at the LHC. (a), (b) and (c) are the fully elastic, semi elastic and fully inelastic contributions to the $\gamma\gamma$ fusion production respectively. (d) The quark-antiquark initiated production of ϕ in association with a photon.

Production mode	$\gamma\gamma \to \phi$	$\gamma p \to \phi j$	$pp \to \phi jj$	$pp \to \phi\gamma$	$pp \to \phi\gamma j$	$pp \to \phi\gamma jj$
CS@8TeV (fb)	32.18	7.841	0.451	0.182	0.095	0.043
CS@13TeV (fb)	110.5	29.94	1.846	1.116	0.711	0.396

TABLE II. Partonic cross sections of various production channels of ϕ for $M_\phi = 1$ TeV and $\Lambda = 2$ TeV computed at renormalization (μ_R) and factorization (μ_F) scales $\mu_R = \mu_F = M_\phi = 1$ TeV for the LHC at 8 and 13 TeV. These cross sections are computed using MMHT14LO PDFs by applying some basic generation level cuts as defined in Eq. (15). Here, p includes b-quark PDF and j denotes light jets including b-jet. All signal cross sections scale as Λ^{-2}.

basic kinematical cuts at the generation level wherever they are applicable.

$$p_T(x) > 25 \text{ GeV}; \quad |\eta(x)| < 2.5; \quad \Delta R(x,y) > 0.4 \quad \text{where} \quad x, y \equiv \{\gamma, j\} \tag{15}$$

In our analysis, we include inelastic, semi-elastic and elastic contributions (as shown in Fig. 3) in the $\gamma\gamma$ fusion process. In order to include these three contributions properly without double counting, we use the MLM matching algorithm [144] to match matrix element partons with the parton shower to generate inclusive $pp \to \phi$ signal events. Our inclusive signal includes up to two jets and we generate it by combining the following processes,

$$\left.\begin{aligned} \gamma\gamma &\to (\phi) &&\to \widehat{\gamma\gamma}, \\ \gamma p &\to (\phi\, j) &&\to \widehat{\gamma\gamma}\, j\,, \\ pp &\to (\phi\, jj) &&\to \widehat{\gamma\gamma}\, jj\,. \end{aligned}\right\} \tag{16}$$

where we set the matching scale $Q_{cut} = 125$ GeV and the curved connection above two photons signify that they come from the decay of ϕ. To determine the appropriate Q_{cut} for the process, we check the smooth transition in differential jet rate distributions between events with N and $N+1$ jets. Moreover, variations of Q_{cut} around 125 GeV would not change the matched cross section much which we ensured to be within $\sim 10\%$ of the zero jet contribution. The matched cross section of the inclusive (up to 2-jets) $pp \to \phi +$ jets process is roughly 64 (20) fb for 13 (8) TeV LHC and includes the $\phi \to \gamma\gamma$ BR. For a TeV-scale resonance the $\gamma\gamma \to \phi \to \gamma\gamma$ with parton shower contribution is very similar to the total matched cross sections. Therefore, one can use just $\gamma\gamma$ process in a simplified analysis for a high mass resonance. We also generate inclusive $pp \to \phi\gamma$ (up to 2-jets) events by using similar matching technique. This channel has an interesting final state

with three hard photons. In most events, the first and second hardest photons come from ϕ-decay, and their transverse momentum (p_T) distributions roughly peak around $M_\phi/2$, as they come from the decay of ϕ. We observe that the third photon, although relatively softer than the first two, is also moderately hard. When one constructs the invariant mass (M) of the two hardest photons, the third photon would not contaminate much. As a result, we observe a sharp peak around M_ϕ in the invariant mass distribution of the first and second hardest photons $M(\gamma\gamma)$. Therefore, this channel can provide an interesting signature with three hard photons with $M(\gamma\gamma)$ of first two peaking at M_ϕ.

There is another channel $pp \to \phi \to \gamma\ell\ell$ (where $\ell = \{e, \mu\}$) which might also be interesting to search for as the BR of ϕ to $\gamma\ell\ell$ mode is relatively big and also very clean final state. But since the two leptons are coming from an off-shell photon, they are not spatially very separated and therefore a dedicated analysis is required to observe this channel. Similar analyses for the SM Higgs have been done previously for the LHC [145].

IV. EXCLUSION FROM THE LHC DATA

Run-I and run-II LHC data on the diphoton resonance searches set strong upper limits (UL) on $\sigma \times \text{BR}$. It should be remembered that all these searches are generally optimized for an s-channel resonance (spin-0 or spin-2) produced through gg fusion and decaying to two photons. For exclusive searches, one demands exactly two selected photons with no selected jet, whereas for inclusive searches, one keeps events with at least two selected photons and any number of selected jets. In order to derive a limit on Λ by recasting the $\sigma \times \text{BR}$ UL from an experiment, we need to properly take care of the cut efficiencies. The cut efficiencies can significantly change for different selection criteria and also for different production mechanisms. For instance, in our case, the scalar is dominantly produced through $\gamma\gamma$ fusion and the signal cut efficiency can be different from gg fusion production. This can be properly taken care of by using the following relation:

$$\mathcal{N}_s = \sigma_s \times \epsilon_s \times \mathcal{L} = \left(\sum_i \sigma_i \times \epsilon_i \right) \times \mathcal{L} \ , \tag{17}$$

where $\mathcal{N}_s$ is the number of events for the signal considered and σ_s is the corresponding signal cross section for luminosity $\mathcal{L}$. The corresponding signal cut efficiency is denoted by ϵ_s. When different types of signal topology and/or final state contribute to any

experimental observable, $\mathcal{N}_s$ can be expressed by the sum $(\sum_i \sigma_i \times \epsilon_i) \times \mathcal{L}$. Here, i runs over all contributing signal processes to any observable.

We roughly employ the selection cuts used by ATLAS [7] and CMS [8] for their 13 TeV analyses as listed below. Although they have not mentioned any jet selection, we include basic jet selection cuts in the following list to demonstrate how our signal cut efficiencies change with different number of selected photons and jets.

- Selection cuts for ATLAS 13 TeV analysis:

  1. Transverse momentum of the selected photons and jets satisfy $p_T(\gamma), p_T(j) > 25$ GeV.
  2. Pseudorapidity of the selected photons satisfy $|\eta(\gamma)| < 2.37$ excluding the barrel-endcap region $1.37 < |\eta(\gamma)| < 1.52$ and jets $|\eta(j)| < 4.4$.
  3. Separation in η-ϕ plane between any two photons or photon-jet pair satisfies $\Delta R(\gamma, \gamma), \Delta R(\gamma, j) > 0.4$.
  4. Invariant mass of the two hardest photons and their transverse momenta satisfy the relations $p_T(\gamma_1)/M(\gamma_1, \gamma_2) > 0.4$ and $p_T(\gamma_2)/M(\gamma_1, \gamma_2) > 0.3$.

- Selection cuts for CMS 13 TeV analysis:

  1. Transverse momentum of the selected photons and jets satisfy $p_T(\gamma), p_T(j) > 25$ GeV with two hardest photons satisfying $p_T(\gamma_1), p_T(\gamma_2) > 75$ GeV.
  2. Pseudorapidity of the selected photons satisfy $|\eta(\gamma)| < 2.5$ excluding the barrel-endcap region $1.44 < |\eta(\gamma)| < 1.57$ (and rejecting events with both photons are in endcap region) and jets $|\eta(j)| < 4.5$.
  3. Separation in η-ϕ plane between any two photons or photon-jet pair satisfies $\Delta R(\gamma, \gamma), \Delta R(\gamma, j) > 0.4$.
  4. Invariant mass of the two hardest photons satisfies $M(\gamma_1, \gamma_2) > 230$ GeV and $M(\gamma_1, \gamma_2) > 320$ GeV for events with at least one photon is in endcap region.

Now, we want to investigate how selection cut efficiencies depend on the different selection criteria imposed on the number of photons and jets. In Table III, we show

Category	$2\gamma+\geq 0j$	$2\gamma+\geq 1j$	$2\gamma+\geq 2j$	$\geq 2\gamma+\geq 0j$	$\geq 3\gamma+\geq 0j$
CMS ($\phi\to\gamma\gamma$)	0.679	0.277	0.100	0.682	0.002
CMS ($\phi\gamma\to 3\gamma$)	0.270	0.249	0.180	0.931	0.662
ATLAS ($\phi\to\gamma\gamma$)	0.475	0.192	0.069	0.476	0.001
ATLAS ($\phi\gamma\to 3\gamma$)	0.227	0.202	0.142	0.769	0.541

TABLE III. Cut efficiencies for different selection criteria on the number of selected photons and jets for the 13 TeV ATLAS [7] and CMS [8] diphoton resonance searches. Here, we use inclusive (up to 2-jets) $pp\to\phi\gamma\to 3\gamma$ and $pp\to\phi jj\to\gamma\gamma jj$ processes for the analysis.

cut efficiencies for different selection criteria on the number of photons and jets for the inclusive $pp\to\phi\to\gamma\gamma$ and $pp\to\phi\gamma\to 3\gamma$ channels at the 13 TeV LHC.

From Table III, it is evident that the cut efficiencies are highly dependent on the selection criteria. For example, if we demand exactly two selected photons and any number of jets (i.e., $2\gamma+\geq 0j$), the cut efficiency is 68% for CMS ($\phi\to\gamma\gamma$). On the other hand, this becomes 28% when we select two photons and at least one jet (i.e., $2\gamma+\geq 1j$). This is in contrast to the case of an s-channel production of SM-like scalar through gg fusion decays to two photons, where we should not expect drastically different cut efficiencies for $2\gamma+\geq 0j$ and $2\gamma+\geq 1j$ selection categories. This is because due to the presence of gluons in the initial state, radiation of jets will be more compared to photon initiated process and therefore in most of the events one would expect at least one additional jet.

In our model, ϕ is dominantly produced from $\gamma\gamma$ fusion, but in many BSM theories, a TeV-scale scalar can be dominantly produced from gg fusion, just like the SM Higgs. If it is produced from gg fusion, due to the presence of colored particle in the initial state, the jet activities is expected to be different from that in $\gamma\gamma$ fusion production. Therefore, some jet observables like jet multiplicity, pseudorapidity, or transverse momentum distributions of jets can act as good discriminating variables to distinguish different production mechanisms. In Fig. 4a, we show the jet multiplicity distribution for ϕ produced from $\gamma\gamma$ fusion for the $2\gamma+\geq 0j$ selection category. In Figs. 4b and 4c, we show the η and p_T distributions of the hardest jet for the $2\gamma+\geq 1j$ category. In context of 750 GeV diphoton excess, the issue to distinguish different production mechanisms by analyzing

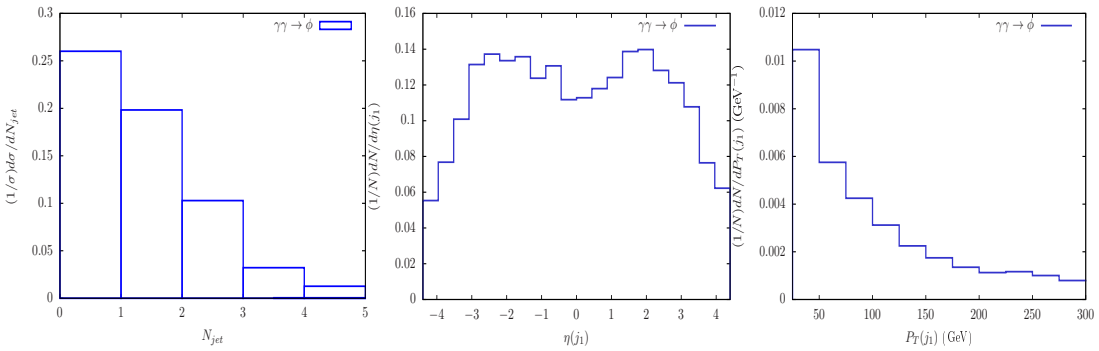

(a) (b) (c)

FIG. 4. For the inclusive $pp \to \phi$ process: (a) jet multiplicity distribution for the $2\gamma+ \geq 0j$ category and, (b) pseudorapidity distribution and (c) transverse momentum distribution for the hardest jet for $2\gamma+ \geq 1j$ category. These distributions are drawn after selecting events by applying 13 TeV ATLAS cuts as defined earlier.

various kinematic distributions are discussed in Refs. [107, 146–151].

Now we turn to the 8 TeV LHC data related to the diphoton resonance searches [152–154]. All these experiments search for either a spin-0 or spin-2 object produced through gg fusion decaying to two photons. We collect the observed upper limit on the cross sections and the corresponding efficiencies for resonance mass around 1 TeV for each experiment. We estimate the cut efficiencies for the process $pp \to \phi \to \gamma\gamma$ for these experiments by employing selection cuts in the detector simulator DELPHES3. From this information, one can estimate the lower limit on Λ from the formula given in Eq. (17). The overall result from ATLAS and CMS set an upper limit of the cross section roughly 1 fb for 1 TeV resonance mass. Using this we can extract a lower limit on Λ for our model. This depends, however, on how the data is characterized in terms of number of photons and jets, since that affects the relevant cut efficiencies. Without reporting all numerical details here, we conclude that for the interpretation of the data as $2\gamma+ \geq 0j$, we obtain a lower limit of Λ in the range $8.5 - 9$ TeV for $M_\phi = 1$ TeV. Choosing instead $2\gamma+ \geq 1j$ would, however, give a lower limit Λ in the range $4.5 - 5$ TeV. There is another relevant experiment at the 8 TeV LHC by ATLAS with $\mathcal{L} = 20.3$ fb^{-1} which is important to mention in this context. In [155], a triphoton resonance is searched for by ATLAS. This analysis is limited up to a resonance mass of 500 GeV. In our model, there is a possibility of a three photon final state originating from $pp \to \phi\gamma \to 3\gamma$ (although not a

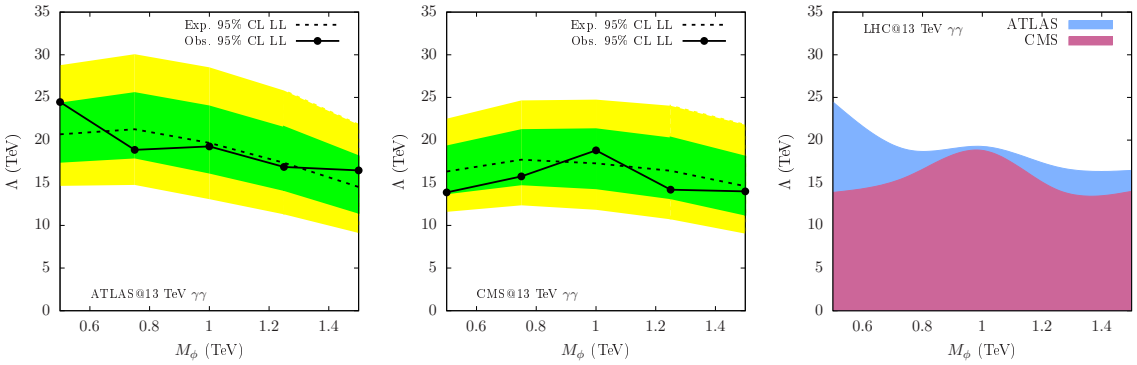

(a) (b) (c)

FIG. 5. The derived lower limits (LL) on Λ as functions of M_ϕ by recasting the UL on $\sigma \times$ BR as set by (a) ATLAS and (b) CMS diphoton resonance searches at the 13 TeV LHC. The black dashed and solid curves are expected and observed limits respectively. The green and yellow bands correspond to 1σ and 2σ uncertainty associated to the expected limits. (c) The shaded regions are excluded from the observed data.

triphoton resonance), and therefore, triphoton resonance searches can also be used to set limits on our model parameters in the future, if the analysis extends the resonance mass range beyond 1 TeV.

The latest 13 TeV LHC data on the diphoton resonance searches also set strong upper limit on $\sigma \times \text{BR} \sim 1$ fb for a diphoton resonance mass of around 1 TeV. Following the same method as used to derive limits on Λ from the 8 TeV data, we obtain stronger limits on Λ. As mentioned earlier, the extraction of Λ depends on what selection category is used. For the category of $2\gamma+ \geq 0j$ selection for ATLAS and CMS analyses, we get $\Lambda \sim 18$ TeV for $M_\phi = 1$ TeV. On the other hand we get slightly smaller $\Lambda \sim 12$ TeV for the selection category $2\gamma+ \geq 1j$. In Fig. 5, we show the derived limits on Λ as functions of M_ϕ using latest ATLAS and CMS diphoton resonance search data at 13 TeV.

Finally we wish to briefly discuss the general varying EW theory, which we introduced in Section II, in light of the LHC data. In Table I, we see that the BR for $\phi \to \gamma\gamma$ is about 62% for $M_\phi = 1$ TeV when only the variation of the EM coupling is considered. For the varying EW theory, this BR will reduce due to the appearance of other two-body decay modes. For instance, for $\alpha = 1$ and $\beta = 0$ in Eq. (11), the BR for $\phi \to \gamma\gamma$ becomes 37%. One should note that this BR reduction does not lower Λ drastically, since the production cross section scales as Λ^{-2}. For this particular benchmark, the derived Λ will

reduce by a factor $\sqrt{0.6} \approx 0.77$. For example, $\Lambda \lesssim 18$ TeV for $M_\phi = 1$ TeV as shown in Fig. 5 will become 14 TeV.

It is also necessary to check how the latest 13 TeV LHC data on the $\gamma\gamma$, γZ and ZZ resonance searches place bounds on Λ for the varying EW theory. The 13 TeV data set rough upper limits on the cross sections for $\gamma\gamma$, γZ and ZZ resonance searches around mass 1 TeV as 1 fb [7, 8], 10 fb [131, 132] and 20 fb [133], respectively. Since the limits on the cross sections for γZ and ZZ resonance searches are milder than the $\gamma\gamma$ limit, they cannot put stronger bounds than that derived from $\gamma\gamma$ data as the $\gamma\gamma$ BR is the largest for $\alpha = 1$ and $\beta = 0$ benchmark in Eq. (13).

V. CONCLUSIONS

In this paper, we present the first ever study of the phenomenology of a heavy scalar associated with the variation of the fine-structure constant. This variation introduces a new scalar field in the theory as originally proposed by Jacob Bekenstein. We introduce a TeV-scale mass of the scalar which can therefore be accessible at the LHC. This model predicts that the scalar dominantly couples to photons. Therefore, the dominant production channel is $\gamma\gamma$ fusion and it dominantly decays to a photon pair. The scalar can also be produced together with an additional real or virtual photon, which, if virtual, gives rise to a pair of jets or leptons. This gives another prediction: the existence of an additional photon or jets in the events, which are not part of the resonance. These predictions can be searched for in the future at the LHC.

The model we study here is very economical and has only two new parameters, the mass of the scalar M_ϕ and the energy scale Λ. We use latest 13 TeV LHC diphoton resonance search data to derive exclusion regions on the $M_\phi - \Lambda$ plane. In particular, for the mass $M_\phi \sim 1$ TeV, we obtain a lower limit of 18 TeV on Λ. We also discuss how different selection criteria can affect the exclusion limits and derive limits from relevant LHC data for different selection categories. For simplicity in this first paper, we mostly consider varying only $\alpha_{\rm EM}$ in the SM and resulting phenomenology at the LHC. The variations of gauge couplings in the full electroweak theory leads to more complex possibilities, which we briefly discuss and derive limits for a specific benchmark point. In a forthcoming paper, we further investigate the phenomenology of varying couplings in

the full electroweak theory.

In a broader perspective, one should note that the interaction terms for the new scalar are non-renormalizable such that the theory needs to be UV-completed with new physics at the energy scale Λ. The scalar in our model could then be interpreted as a moduli field parametrizing a varying electromagnetic coupling. Natural candidates for such new physics are extra dimensions or string theory, with effects that may be within reach of the LHC.

ACKNOWLEDGMENTS

We thank Elin Bergeaas Kuutmann and Richard Brenner for helpful discussions and the anonymous referees for constructive criticism. This work is supported by the Swedish Research Council (contracts 621-2011-5107 and 2015-04814) and the Carl Trygger Foundation (contract CTS-14:206).

---

[1] J. D. Bekenstein, Phys. Rev. **D25**, 1527 (1982).

[2] J. D. Bekenstein, Phys. Rev. **D66**, 123514 (2002), arXiv:gr-qc/0208081 [gr-qc].

[3] J.-P. Uzan, Living Rev. Rel. **14**, 2 (2011), arXiv:1009.5514 [astro-ph.CO].

[4] M. Zagermann, *Proc. Symposium From Varying Couplings to Fundamental Physics, JENAM 2010*, Astrophys. Space Sci. Proc. , 17 (2011).

[5] ATLAS Collaboration, *Search for resonances decaying to photon pairs in 3.2 fb^{-1} of pp collisions at $\sqrt{s}$ = 13 TeV with the ATLAS detector*, Tech. Rep. ATLAS-CONF-2015-081 (2015).

[6] CMS Collaboration, *Search for new physics in high mass diphoton events in proton-proton collisions at 13TeV*, Tech. Rep. CMS-PAS-EXO-15-004 (2015).

[7] T. A. collaboration (ATLAS), (2016).

[8] V. Khachatryan *et al.* (CMS), (2016), arXiv:1609.02507 [hep-ex].

[9] Y. Mambrini, G. Arcadi, and A. Djouadi, (2015), arXiv:1512.04913 [hep-ph].

[10] M. Backovic, A. Mariotti, and D. Redigolo, (2015), arXiv:1512.04917 [hep-ph].

[11] A. Angelescu, A. Djouadi, and G. Moreau, (2015), arXiv:1512.04921 [hep-ph].

[12] Y. Nakai, R. Sato, and K. Tobioka, (2015), arXiv:1512.04924 [hep-ph].

[13] A. Pilaftsis, (2015), arXiv:1512.04931 [hep-ph].

[14] T. Higaki, K. S. Jeong, N. Kitajima, and F. Takahashi, (2015), arXiv:1512.05295 [hep-ph].

[15] S. D. McDermott, P. Meade, and H. Ramani, (2015), arXiv:1512.05326 [hep-ph].

[16] J. Ellis, S. A. R. Ellis, J. Quevillon, V. Sanz, and T. You, (2015), arXiv:1512.05327 [hep-ph].

[17] M. Low, A. Tesi, and L.-T. Wang, (2015), arXiv:1512.05328 [hep-ph].

[18] B. Bellazzini, R. Franceschini, F. Sala, and J. Serra, (2015), arXiv:1512.05330 [hep-ph].

[19] C. Petersson and R. Torre, (2015), arXiv:1512.05333 [hep-ph].

[20] E. Molinaro, F. Sannino, and N. Vignaroli, (2015), arXiv:1512.05334 [hep-ph].

[21] B. Dutta, Y. Gao, T. Ghosh, I. Gogoladze, and T. Li, (2015), arXiv:1512.05439 [hep-ph].

[22] Q.-H. Cao, Y. Liu, K.-P. Xie, B. Yan, and D.-M. Zhang, (2015), arXiv:1512.05542 [hep-ph].

[23] S. Matsuzaki and K. Yamawaki, (2015), arXiv:1512.05564 [hep-ph].

[24] A. Kobakhidze, F. Wang, L. Wu, J. M. Yang, and M. Zhang, (2015), arXiv:1512.05585 [hep-ph].

[25] R. Martinez, F. Ochoa, and C. F. Sierra, (2015), arXiv:1512.05617 [hep-ph].

[26] P. Cox, A. D. Medina, T. S. Ray, and A. Spray, (2015), arXiv:1512.05618 [hep-ph].

[27] D. Becirevic, E. Bertuzzo, O. Sumensari, and R. Z. Funchal, (2015), arXiv:1512.05623 [hep-ph].

[28] J. M. No, V. Sanz, and J. Setford, (2015), arXiv:1512.05700 [hep-ph].

[29] S. V. Demidov and D. S. Gorbunov, (2015), arXiv:1512.05723 [hep-ph].

[30] W. Chao, R. Huo, and J.-H. Yu, (2015), arXiv:1512.05738 [hep-ph].

[31] D. Curtin and C. B. Verhaaren, (2015), arXiv:1512.05753 [hep-ph].

[32] L. Bian, N. Chen, D. Liu, and J. Shu, (2015), arXiv:1512.05759 [hep-ph].

[33] J. Chakrabortty, A. Choudhury, P. Ghosh, S. Mondal, and T. Srivastava, (2015), arXiv:1512.05767 [hep-ph].

[34] A. Ahmed, B. M. Dillon, B. Grzadkowski, J. F. Gunion, and Y. Jiang, (2015), arXiv:1512.05771 [hep-ph].

[35] P. Agrawal, J. Fan, B. Heidenreich, M. Reece, and M. Strassler, (2015), arXiv:1512.05775 [hep-ph].

[36] D. Aloni, K. Blum, A. Dery, A. Efrati, and Y. Nir, (2015), arXiv:1512.05778 [hep-ph].

[37] Y. Bai, J. Berger, and R. Lu, (2015), arXiv:1512.05779 [hep-ph].

[38] E. Gabrielli, K. Kannike, B. Mele, M. Raidal, C. Spethmann, and H. Veermae, (2015), arXiv:1512.05961 [hep-ph].

[39] R. Benbrik, C.-H. Chen, and T. Nomura, (2015), arXiv:1512.06028 [hep-ph].

[40] A. Alves, A. G. Dias, and K. Sinha, (2015), arXiv:1512.06091 [hep-ph].

[41] E. Megias, O. Pujolas, and M. Quiros, (2015), arXiv:1512.06106 [hep-ph].

[42] L. M. Carpenter, R. Colburn, and J. Goodman, (2015), arXiv:1512.06107 [hep-ph].

[43] W. Chao, (2015), arXiv:1512.06297 [hep-ph].

[44] M. T. Arun and P. Saha, (2015), arXiv:1512.06335 [hep-ph].

[45] C. Han, H. M. Lee, M. Park, and V. Sanz, (2015), arXiv:1512.06376 [hep-ph].

[46] S. Chang, (2015), arXiv:1512.06426 [hep-ph].

[47] I. Chakraborty and A. Kundu, (2015), arXiv:1512.06508 [hep-ph].

[48] R. Ding, L. Huang, T. Li, and B. Zhu, (2015), arXiv:1512.06560 [hep-ph].

[49] H. Han, S. Wang, and S. Zheng, (2015), arXiv:1512.06562 [hep-ph].

[50] X.-F. Han and L. Wang, (2015), arXiv:1512.06587 [hep-ph].

[51] M.-x. Luo, K. Wang, T. Xu, L. Zhang, and G. Zhu, (2015), arXiv:1512.06670 [hep-ph].

[52] J. Chang, K. Cheung, and C.-T. Lu, (2015), arXiv:1512.06671 [hep-ph].

[53] D. Bardhan, D. Bhatia, A. Chakraborty, U. Maitra, S. Raychaudhuri, and T. Samui, (2015), arXiv:1512.06674 [hep-ph].

[54] T.-F. Feng, X.-Q. Li, H.-B. Zhang, and S.-M. Zhao, (2015), arXiv:1512.06696 [hep-ph].

[55] O. Antipin, M. Mojaza, and F. Sannino, (2015), arXiv:1512.06708 [hep-ph].

[56] F. Wang, L. Wu, J. M. Yang, and M. Zhang, (2015), arXiv:1512.06715 [hep-ph].

[57] J. Cao, C. Han, L. Shang, W. Su, J. M. Yang, and Y. Zhang, (2015), arXiv:1512.06728 [hep-ph].

[58] F. P. Huang, C. S. Li, Z. L. Liu, and Y. Wang, (2015), arXiv:1512.06732 [hep-ph].

[59] W. Liao and H.-q. Zheng, (2015), arXiv:1512.06741 [hep-ph].

[60] J. J. Heckman, (2015), arXiv:1512.06773 [hep-ph].

[61] M. Dhuria and G. Goswami, (2015), arXiv:1512.06782 [hep-ph].

[62] X.-J. Bi, Q.-F. Xiang, P.-F. Yin, and Z.-H. Yu, (2015), arXiv:1512.06787 [hep-ph].

[63] J. S. Kim, K. Rolbiecki, and R. R. de Austri, (2015), arXiv:1512.06797 [hep-ph].

[64] W. S. Cho, D. Kim, K. Kong, S. H. Lim, K. T. Matchev, J.-C. Park, and M. Park, (2015), arXiv:1512.06824 [hep-ph].

[65] J. M. Cline and Z. Liu, (2015), arXiv:1512.06827 [hep-ph].

[66] M. Bauer and M. Neubert, (2015), arXiv:1512.06828 [hep-ph].

[67] K. Kulkarni, (2015), arXiv:1512.06836 [hep-ph].

[68] S. M. Boucenna, S. Morisi, and A. Vicente, (2015), arXiv:1512.06878 [hep-ph].

[69] C. W. Murphy, (2015), arXiv:1512.06976 [hep-ph].

[70] A. E. C. Hernandez and I. Nisandzic, (2015), arXiv:1512.07165 [hep-ph].

[71] U. K. Dey, S. Mohanty, and G. Tomar, (2015), arXiv:1512.07212 [hep-ph].

[72] G. M. Pelaggi, A. Strumia, and E. Vigiani, (2015), arXiv:1512.07225 [hep-ph].

[73] J. de Blas, J. Santiago, and R. Vega-Morales, (2015), arXiv:1512.07229 [hep-ph].

[74] A. Belyaev, G. Cacciapaglia, H. Cai, T. Flacke, A. Parolini, and H. Serodio, (2015), arXiv:1512.07242 [hep-ph].

[75] P. S. B. Dev and D. Teresi, (2015), arXiv:1512.07243 [hep-ph].

[76] W.-C. Huang, Y.-L. S. Tsai, and T.-C. Yuan, (2015), arXiv:1512.07268 [hep-ph].

[77] S. Moretti and K. Yagyu, (2015), arXiv:1512.07462 [hep-ph].

[78] K. M. Patel and P. Sharma, (2015), arXiv:1512.07468 [hep-ph].

[79] M. Badziak, (2015), arXiv:1512.07497 [hep-ph].

[80] S. Chakraborty, A. Chakraborty, and S. Raychaudhuri, (2015), arXiv:1512.07527 [hep-ph].

[81] Q.-H. Cao, S.-L. Chen, and P.-H. Gu, (2015), arXiv:1512.07541 [hep-ph].

[82] W. Altmannshofer, J. Galloway, S. Gori, A. L. Kagan, A. Martin, and J. Zupan, (2015), arXiv:1512.07616 [hep-ph].

[83] M. Cvetic, J. Halverson, and P. Langacker, (2015), arXiv:1512.07622 [hep-ph].

[84] J. Gu and Z. Liu, (2015), arXiv:1512.07624 [hep-ph].

[85] B. C. Allanach, P. S. B. Dev, S. A. Renner, and K. Sakurai, (2015), arXiv:1512.07645 [hep-ph].

[86] H. Davoudiasl and C. Zhang, (2015), arXiv:1512.07672 [hep-ph].

[87] N. Craig, P. Draper, C. Kilic, and S. Thomas, (2015), arXiv:1512.07733 [hep-ph].

[88] K. Das and S. K. Rai, (2015), arXiv:1512.07789 [hep-ph].

[89] K. Cheung, P. Ko, J. S. Lee, J. Park, and P.-Y. Tseng, (2015), arXiv:1512.07853 [hep-ph].

[90] J. Liu, X.-P. Wang, and W. Xue, (2015), arXiv:1512.07885 [hep-ph].

[91] J. Zhang and S. Zhou, (2015), arXiv:1512.07889 [hep-ph].

[92] J. A. Casas, J. R. Espinosa, and J. M. Moreno, (2015), arXiv:1512.07895 [hep-ph].

[93] L. J. Hall, K. Harigaya, and Y. Nomura, (2015), arXiv:1512.07904 [hep-ph].

[94] H. Han, S. Wang, and S. Zheng, (2015), arXiv:1512.07992 [hep-ph].

[95] J.-C. Park and S. C. Park, (2015), arXiv:1512.08117 [hep-ph].

[96] A. Salvio and A. Mazumdar, (2015), arXiv:1512.08184 [hep-ph].

[97] D. Chway, R. Dermisek, T. H. Jung, and H. D. Kim, (2015), arXiv:1512.08221 [hep-ph].

[98] G. Li, Y.-n. Mao, Y.-L. Tang, C. Zhang, Y. Zhou, and S.-h. Zhu, (2015), arXiv:1512.08255 [hep-ph].

[99] M. Son and A. Urbano, (2015), arXiv:1512.08307 [hep-ph].

[100] Y.-L. Tang and S.-h. Zhu, (2015), arXiv:1512.08323 [hep-ph].

[101] H. An, C. Cheung, and Y. Zhang, (2015), arXiv:1512.08378 [hep-ph].

[102] J. Cao, F. Wang, and Y. Zhang, (2015), arXiv:1512.08392 [hep-ph].

[103] F. Wang, W. Wang, L. Wu, J. M. Yang, and M. Zhang, (2015), arXiv:1512.08434 [hep-ph].

[104] C. Cai, Z.-H. Yu, and H.-H. Zhang, (2015), arXiv:1512.08440 [hep-ph].

[105] Q.-H. Cao, Y. Liu, K.-P. Xie, B. Yan, and D.-M. Zhang, (2015), arXiv:1512.08441 [hep-ph].

[106] J. E. Kim, (2015), arXiv:1512.08467 [hep-ph].

[107] J. Gao, H. Zhang, and H. X. Zhu, Eur. Phys. J. **C76**, 348 (2016), arXiv:1512.08478 [hep-ph].

[108] W. Chao, (2015), arXiv:1512.08484 [hep-ph].

[109] X.-J. Bi, R. Ding, Y. Fan, L. Huang, C. Li, T. Li, S. Raza, X.-C. Wang, and B. Zhu, (2015), arXiv:1512.08497 [hep-ph].

[110] F. Goertz, J. F. Kamenik, A. Katz, and M. Nardecchia, (2015), arXiv:1512.08500 [hep-ph].

[111] P. S. B. Dev, R. N. Mohapatra, and Y. Zhang, (2015), arXiv:1512.08507 [hep-ph].

[112] N. Bizot, S. Davidson, M. Frigerio, and J.-L. Kneur, (2015), arXiv:1512.08508 [hep-ph].

[113] L. E. Ibanez and V. Martin-Lozano, (2015), arXiv:1512.08777 [hep-ph].

[114] C.-W. Chiang, M. Ibe, and T. T. Yanagida, (2015), arXiv:1512.08895 [hep-ph].

[115] S. K. Kang and J. Song, (2015), arXiv:1512.08963 [hep-ph].

[116] Y. Hamada, T. Noumi, S. Sun, and G. Shiu, (2015), arXiv:1512.08984 [hep-ph].

[117] X.-J. Huang, W.-H. Zhang, and Y.-F. Zhou, (2015), arXiv:1512.08992 [hep-ph].

[118] S. Kanemura, K. Nishiwaki, H. Okada, Y. Orikasa, S. C. Park, and R. Watanabe, (2015), arXiv:1512.09048 [hep-ph].

[119] S. Kanemura, N. Machida, S. Odori, and T. Shindou, (2015), arXiv:1512.09053 [hep-ph].

[120] P. V. Dong and N. T. K. Ngan, (2015), arXiv:1512.09073 [hep-ph].

[121] I. Low and J. Lykken, (2015), arXiv:1512.09089 [hep-ph].

[122] A. E. C. Hernandez, (2015), arXiv:1512.09092 [hep-ph].

[123] Y. Jiang, Y.-Y. Li, and T. Liu, (2015), arXiv:1512.09127 [hep-ph].

[124] K. Kaneta, S. Kang, and H.-S. Lee, (2015), arXiv:1512.09129 [hep-ph].

[125] L. Marzola, A. Racioppi, M. Raidal, F. R. Urban, and H. Veerme, (2015), arXiv:1512.09136 [hep-ph].

[126] E. Ma, (2015), arXiv:1512.09159 [hep-ph].

[127] A. Dasgupta, M. Mitra, and D. Borah, (2015), arXiv:1512.09202 [hep-ph].

[128] U. Danielsson, R. Enberg, G. Ingelman, and T. Mandal, work in progress (2016).

[129] J. Magueijo, H. B. Sandvik, and T. W. B. Kibble, Phys. Rev. **D64**, 023521 (2001), arXiv:hep-ph/0101155 [hep-ph].

[130] D. Kimberly and J. Magueijo, Phys. Lett. **B584**, 8 (2004), arXiv:hep-ph/0310030 [hep-ph].

[131] C. Collaboration (CMS), (2016).

[132] C. Collaboration (CMS), (2016).

[133] T. A. collaboration (ATLAS), (2016).

[134] A. Alloul, N. D. Christensen, C. Degrande, C. Duhr, and B. Fuks, Comput. Phys. Commun. **185**, 2250 (2014), arXiv:1310.1921 [hep-ph].

[135] J. Alwall, R. Frederix, S. Frixione, V. Hirschi, F. Maltoni, O. Mattelaer, H. S. Shao, T. Stelzer, P. Torrielli, and M. Zaro, JHEP **07**, 079 (2014), arXiv:1405.0301 [hep-ph].

[136] L. A. Harland-Lang, A. D. Martin, P. Motylinski, and R. S. Thorne, Eur. Phys. J. **C75**, 204 (2015), arXiv:1412.3989 [hep-ph].

[137] T. Sjstrand, S. Ask, J. R. Christiansen, R. Corke, N. Desai, P. Ilten, S. Mrenna, S. Prestel, C. O. Rasmussen, and P. Z. Skands, Comput. Phys. Commun. **191**, 159 (2015), arXiv:1410.3012 [hep-ph].

[138] J. de Favereau, C. Delaere, P. Demin, A. Giammanco, V. Lematre, A. Mertens, and M. Selvaggi (DELPHES 3), JHEP **02**, 057 (2014), arXiv:1307.6346 [hep-ex].

[139] M. Cacciari, G. P. Salam, and G. Soyez, Eur. Phys. J. **C72**, 1896 (2012), arXiv:1111.6097 [hep-ph].

[140] M. Cacciari, G. P. Salam, and G. Soyez, JHEP **04**, 063 (2008), arXiv:0802.1189 [hep-ph].

[141] S. Fichet, G. von Gersdorff, and C. Royon, (2015), arXiv:1512.05751 [hep-ph].

[142] C. Csaki, J. Hubisz, and J. Terning, (2015), arXiv:1512.05776 [hep-ph].

[143] L. A. Anchordoqui, I. Antoniadis, H. Goldberg, X. Huang, D. Lust, and T. R. Taylor, (2015), arXiv:1512.08502 [hep-ph].

[144] M. L. Mangano, M. Moretti, F. Piccinini, and M. Treccani, JHEP **01**, 013 (2007), arXiv:hep-ph/0611129 [hep-ph].

[145] A. Pozdnyakov, (2015), arXiv:1601.00790 [hep-ex].

[146] C. Cski, J. Hubisz, S. Lombardo, and J. Terning, Phys. Rev. **D93**, 095020 (2016), arXiv:1601.00638 [hep-ph].

[147] J. Bernon, A. Goudelis, S. Kraml, K. Mawatari, and D. Sengupta, JHEP **05**, 128 (2016), arXiv:1603.03421 [hep-ph].

[148] M. A. Ebert, S. Liebler, I. Moult, I. W. Stewart, F. J. Tackmann, K. Tackmann, and L. Zeune, Phys. Rev. **D94**, 051901 (2016), arXiv:1605.06114 [hep-ph].

[149] M. Dalchenko, B. Dutta, Y. Gao, T. Ghosh, and T. Kamon, Phys. Lett. **B761**, 77 (2016), arXiv:1606.03067 [hep-ph].

[150] L. A. Harland-Lang, V. A. Khoze, M. G. Ryskin, and M. Spannowsky, (2016), arXiv:1606.04902 [hep-ph].

[151] B. Fuks, D. W. Kang, S. C. Park, and M.-S. Seo, Phys. Lett. **B761**, 344 (2016), arXiv:1608.00084 [hep-ph].

[152] V. Khachatryan *et al.* (CMS Collaboration), Phys. Lett. **B750**, 494 (2015), arXiv:1506.02301 [hep-ex].

[153] CMS Collaboration, *Search for High-Mass Diphoton Resonances in pp Collisions at sqrt(s)=8 TeV with the CMS Detector*, Tech. Rep. CMS-PAS-EXO-12-045 (2015).

[154] G. Aad *et al.* (ATLAS Collaboration), Phys. Rev. **D92**, 032004 (2015), arXiv:1504.05511 [hep-ex].

[155] G. Aad *et al.* (ATLAS Collaboration), (2015), arXiv:1509.05051 [hep-ex].